Net charge fluctuation in p-p collisions at $\sqrt{s} = 13$ TeV

Rehmat Singh Chawla,[1] Anurag Abhijit Pendse,[1] Samyak Jain,[1] Pravind Kumar Sharma,[1] Shreyas Patil,[1] Ayush Raj Tarway,[1] Paritosh S Hegde,[1] and Uppala Mukesh[1]

[1] *Indian Institute of Technology Bombay, Mumbai, India*

(Dated: November 24, 2021)

The flucatuations in the net charge of proton-proton collisions at $\sqrt{s} = 13$ TeV, generated by the Pythia 8 Monte Carlo event generator were studied against varying multiplicities using ROOT (CERN). Various functions of the moments of net charge were plotted and analysed, and the results were compared to similar analysis for heavy ion collisions.

CONTENTS

I. INTRODUCTION

We analyzed the fluctuation in the net charge produced in proton-proton collisions against the multiplicity. The collisions were generated using the Pythia 8 Monte Carlo event generator and had centre-of-mass energy $\sqrt{s} = 13$ TeV. The dataset consisted of 2 million data points. We analysed the moments of the net charge against 6 multiplicity classes (hereafter called multiplicity bins), which were 0–20, 20–40, 40–60, 60–80, 80–100, and >100.

We utilised ROOT, the data analysis framework developed by CERN, to analyse the data and plot the graphs. The data consisted of the following variables:

ntrack	The number of charged particles in the collision.
Particle ID (pid)	A number identifying the kind of particle. The sign of pid is the sign of the charge, which we used to identify the positive and negatively charged particles
p_T	The transverse momentum of a particle, i.e. the component perpendicular to the z-axis
η	The pseudorapidity, a Lorentz-invariant quantity. $\eta = ln(cot(\theta/2))$, where θ is the angle between the momentum and the z-axis.

We analysed the results in the range $p_T > 0.5$ GeV/c, so as to mimic the low effectiveness of real detectors for lower pT. This shall be implicit in all calculated variables and plots.

The acceptance region is defined as the range where $|\eta| < 1$. The positive and negative charged particle multiplicities (N_+ and N_-) are obtained from the particles in the acceptance region for any collision. The net charge thus obtained ($= N_+ - N_-$) will be plotted against multiplicity values obtained as the number of charged particles in the non-acceptance region of $|\eta| \geq 1$. This has been done, instead of simply using ntrack for the multiplicity, to prevent an autocorrelation between the net charge and multiplicity

The positive and negative charged particle multiplicities (N_+ and N_-) were obtained from the particles in the region $|\eta| < 1$ (called the acceptance region) for any collision. We also obtained the multiplicity estimator as the multiplicity of charged particles in the region $|\eta| \geq 1$, the non-acceptance region.

The net charge thus obtained ($= N_+ - N_-$) was plotted against this multiplicity estimator. This was done, instead of simply using ntrack for the multiplicity, to prevent an autocorrelation between the observable and multiplicity estimator.

II. RESULTS

Fig 1 shows the multiplicity distribution of charged particles with $|\eta| \geq 1$, while fig 2 shows the same for each of the multiplicity bins separately.

Fig 3 shows the multiplicity distribution of charged particles with $|\eta| < 1$ while fig 4 shows the same for each of the multiplicity bins separately.

Fig 5 compares the multiplicity distributions for $|\eta| \geq 1$ and $|\eta| < 1$ in a 2D histogram, with the colour denoting the number of events - the colour in block (x, y) denotes the number of events with multiplicity x for $|\eta| \geq 1$ and multiplicity y for $|\eta| < 1$.

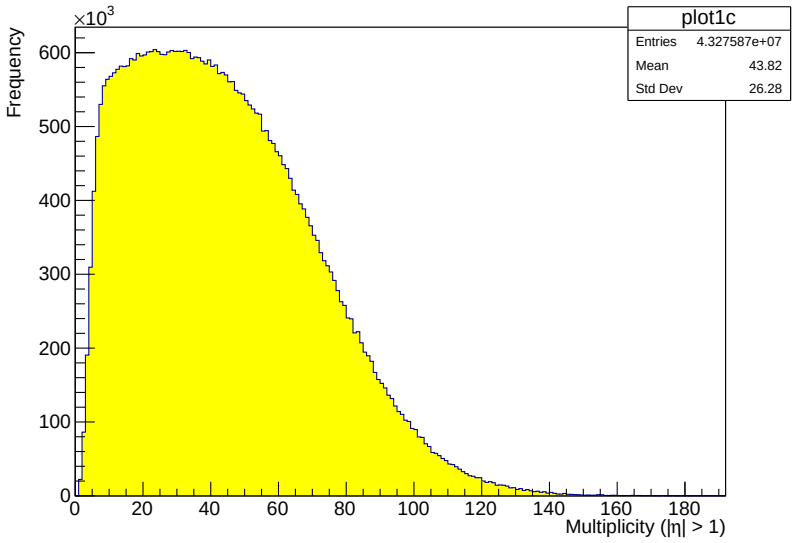

FIG. 1: Multiplicity distribution of charged particles with $|\eta| \geq 1$, all bins combined

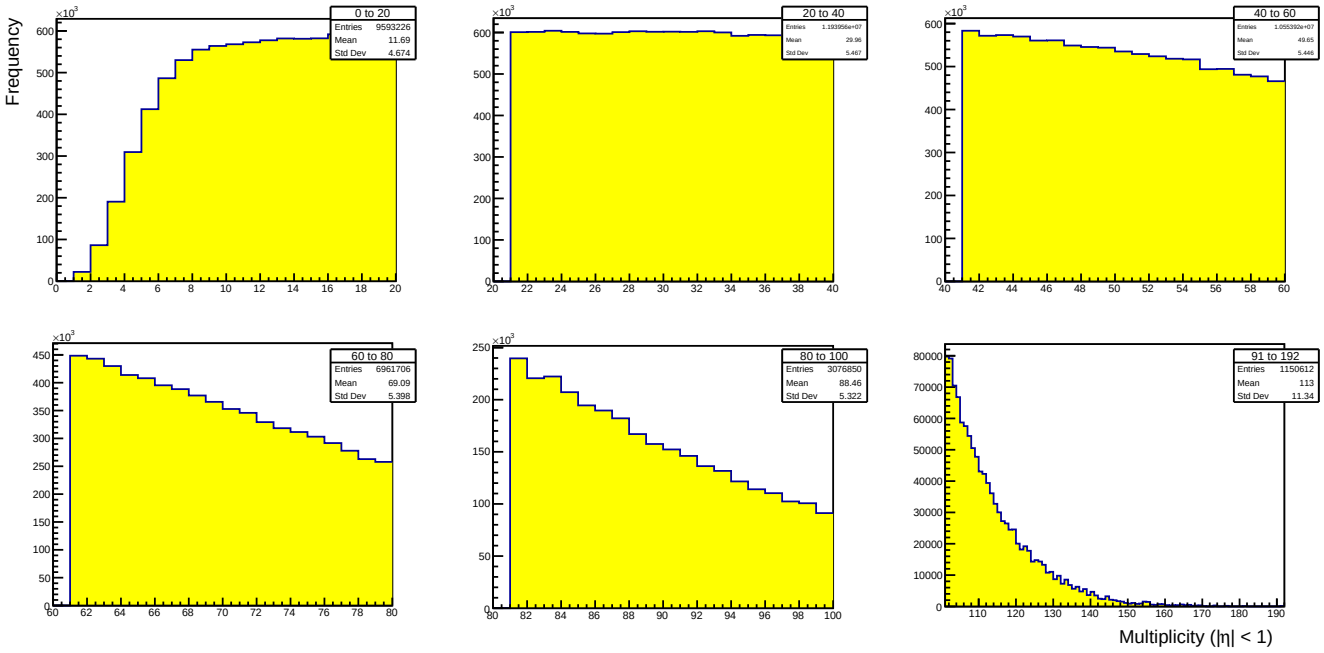

FIG. 2: Multiplicity distribution of charged particles with $|\eta| \geq 1$, all bins separate

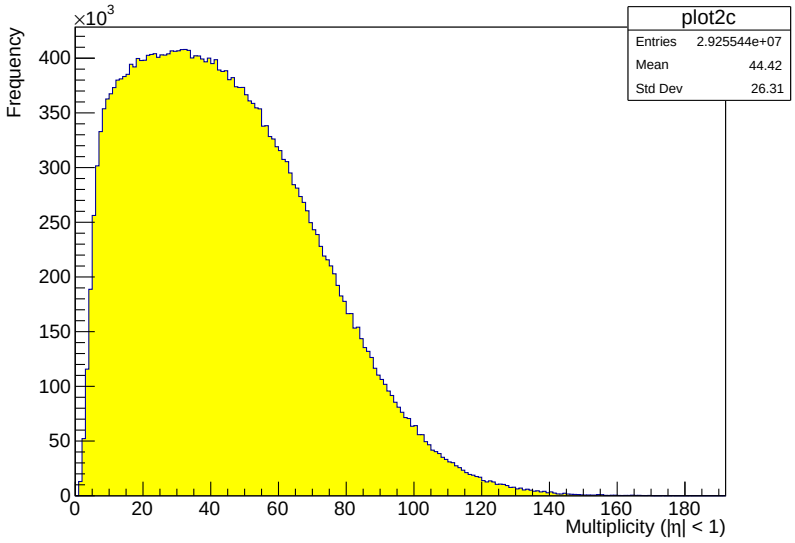

FIG. 3: Multiplicity distribution of charged particles with $|\eta| < 1$, all bins combined

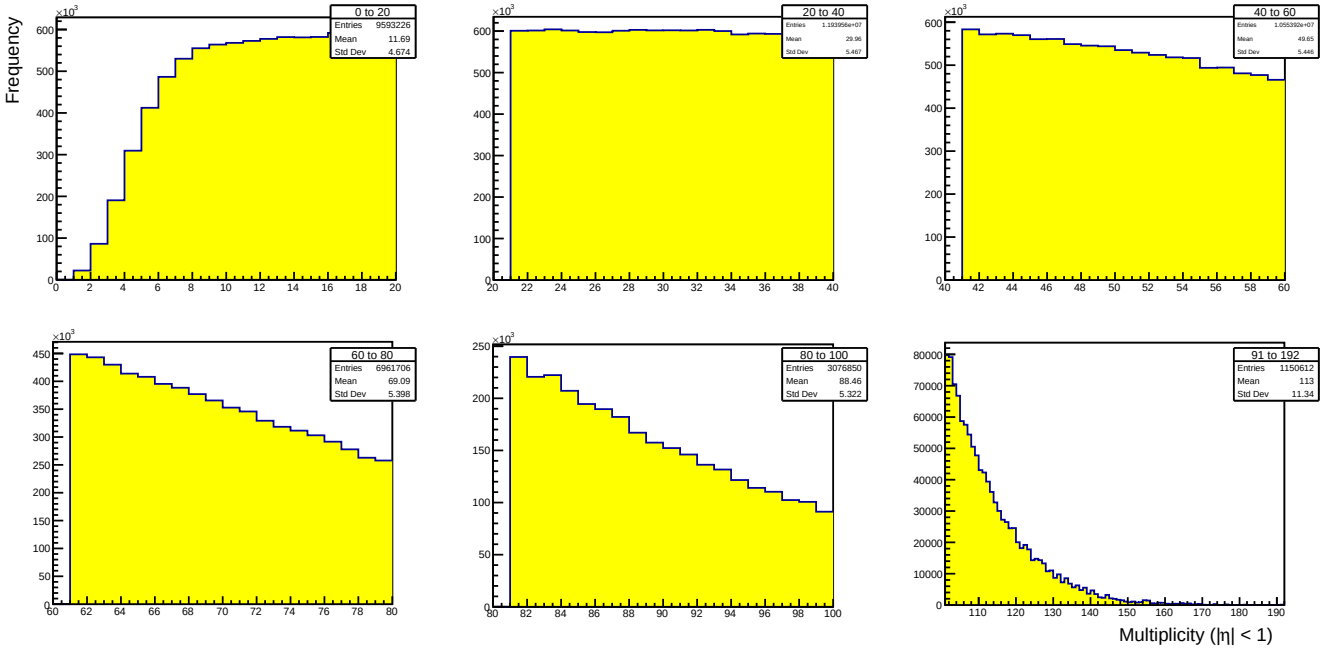

FIG. 4: Multiplicity distribution of charged particles with $|\eta| < 1$, all bins separate

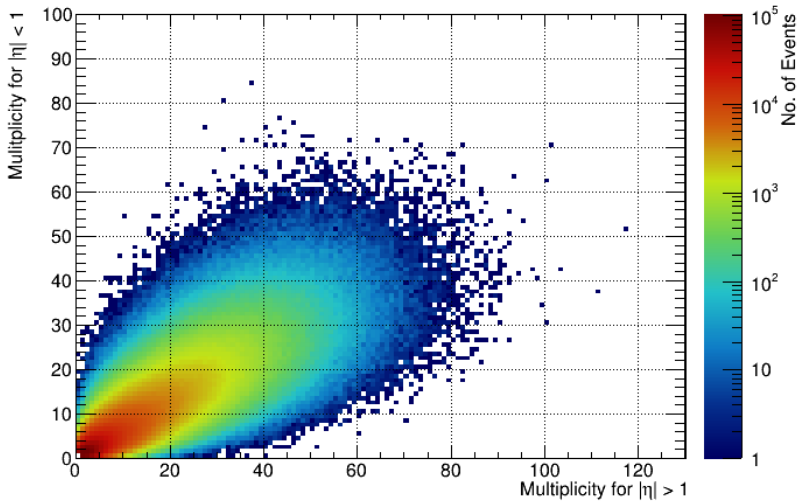

FIG. 5: Frequency against Multiplicity ($|\eta| < 1$) and Multiplicity ($|\eta| \geq 1$), 2D histogram

The variance of the plot along the $x + y = n$ line is a measure of how badly the multiplicity of $|\eta| \geq 1$ suffices as an estimator of some factor of the total multiplicity.

Fig 6 illustrates the net charge values' frequencies against multiplicities ($|\eta| \geq 1$) in a 2D histogram.

Fig 7 is similar, but uses normalised frequencies instead. The normalisation is done such that each total multiplicity bin contributes the same amount to the frequencies as a whole, to offset the effect of the bins 0–20, 20–40 and 40–60 having a much larger number of events than the other 3 bins. The result of this imbalance is that fig 6 is not helpful for interpreting trends in the variances of net charge distributions.

The frequencies are normalised by decreasing the contribution of each event by a factor proportional to the total number of events in the bin the event belongs to.

Thus the normalised frequencies indicate the estimated distributions of the net charges for the case of the dataset consisting of a uniform frequency distribution with respect to the total multiplicities.

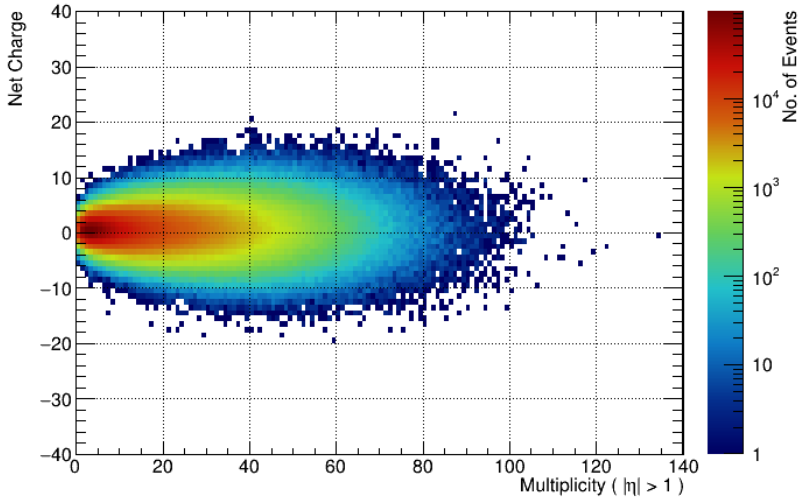

FIG. 6: Frequency against Net Charge and Multiplicity ($|\eta| \geq 1$), 2D histogram

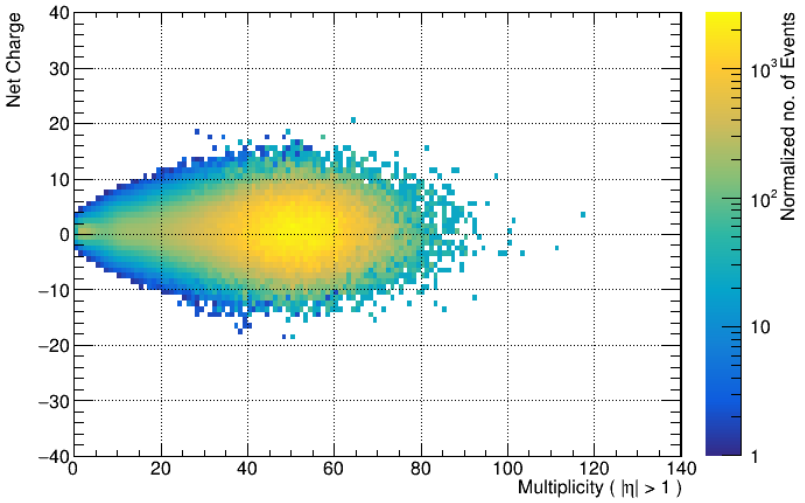

FIG. 7: Normalised frequency against Net Charge and Multiplicity ($|\eta| \geq 1$), 2D histogram

Both graphs illustrate that the net charge distributions all peak close to 0, which is what conservation of charge would dictate. Fig 7 shows that the distribution widens at higher multiplicities, so we expect the variances of net charge distributions to increase with multiplicity.

The unusual pattern for the dark blue boxes can be understood using the results in fig 9b.

In the further graphs, various functions of the moments of net charge distributions are plotted. Instead of a continuous plot against multiplicity, means of the functions for each of the six bins are plotted, against either the midpoint of the bin (labelled "Multiplicity Bins", these are the (a) figures) or against the means of the multiplicity estimator ($|\eta| \geq 1$) values for each of the bins (labelled "Mean Multiplicities", these are the (b) figures).

These functions are the mean (M) (fig 8a, fig 8b), variance (σ^2) (fig 9a, fig 9b), standard deviation (σ) (fig 10a, fig 10b), and two which are scaled variances:

The variance divided by the mean multiplicity (as defined above) for each bin ($\frac{\sigma^2}{M_{\text{mult}}}$) (fig 11a, fig 11b), and variance divided by the mean multiplicity squared ($\frac{\sigma^2}{M^2_{\text{mult}}}$) (fig 12a, fig 12b).

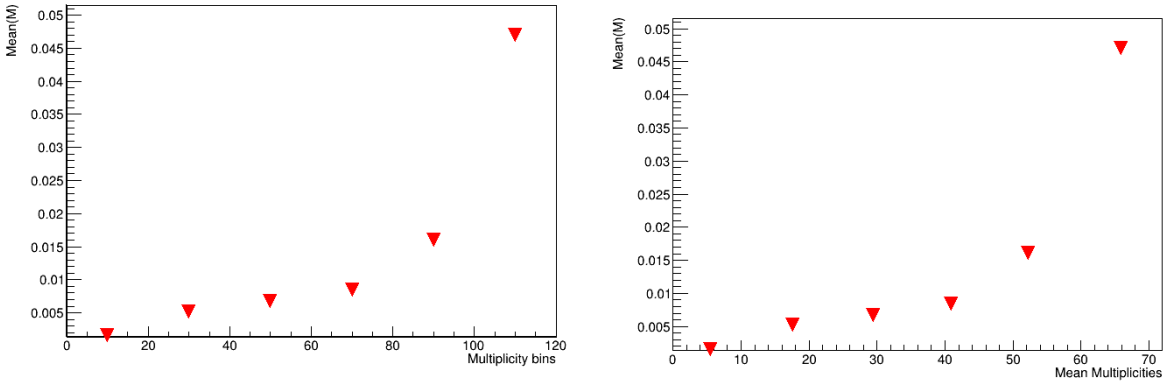

(a) Against Multiplicity bin midpoints

(b) Against mean of Multiplicity ($|\eta| \geq 1$) for each bin

FIG. 8: Mean of Net Charge distributions

The mean of the net charge rises almost linearly with respect to the multiplicity for a the first 4 bins, and then begins to climb rapidly. However, we have a smaller number of datapoints for the multiplicity bin >100, which is the bin which most strongly suggests non-linear behaviour. Hence, further analysis at higher multiplicities and with more datapoints for the same is required to form a conclusion.

It is worth noting that the results of similar analysis done for heavy ion (Au-Au) collisions in the reference show the mean of net charge behaving linearly with respect to the number of participating nucleons.

The means are all positive, and all very small - since the units of net charge are e, even the highest mean is $1/20^{\text{th}}$ the charge of a proton.

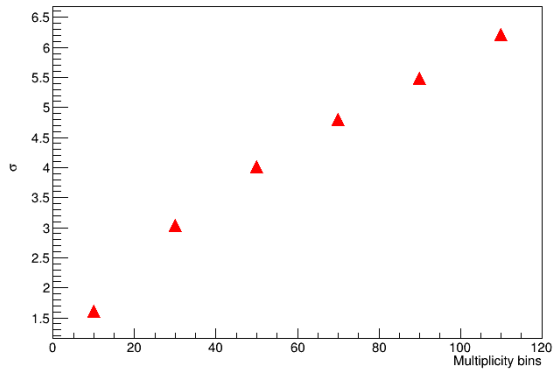

(a) Against Multiplicity bin midpoints

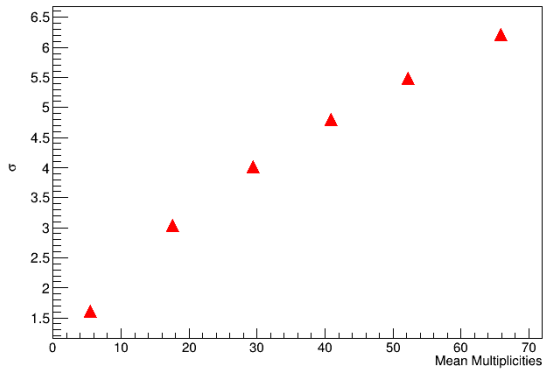

(b) Against mean of Multiplicity ($|\eta| \geq 1$) for each bin

FIG. 9: Standard Deviation of Net Charge distributions

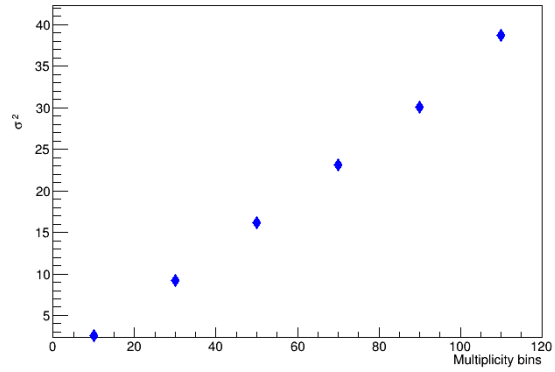

(a) Against Multiplicity bin midpoints

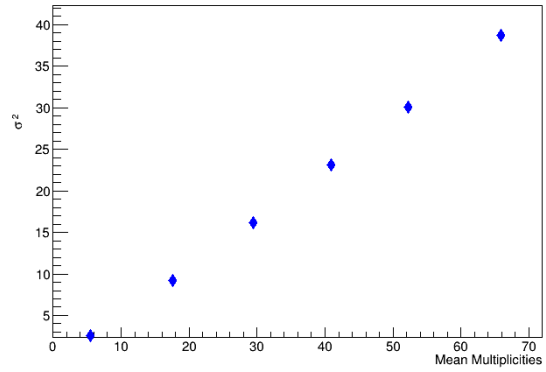

(b) Against mean of Multiplicity ($|\eta| \geq 1$) for each bin

FIG. 10: Variance of Net Charge distributions

The variance of net charge obeys a linear trend with respect to multiplicity, whereas the standard deviation's trend seems slightly concave - which is to be expected, since SD $= \sqrt{\text{Var}}$.

This allows us to explain the unusual pattern for the dark blue coloured boxes in fig 7. As the standard deviation increases with multiplicity, the frequencies of larger magnitudes of net charge tend to increase. However, the lower number of events for the higher multiplicity bins results in a smaller total number of outliers, events with an unusually high magnitude of net charge.

For the lower bins, the number of events is huge, so despite the lower standard deviation causing most of the events to have very low magnitudes of net charge, there is a larger amount of outliers. An outlier in any box means that box will not be white, but rather a dark blue, because there are observations but a very low amount.

Hence, it is non-uniform distribution of events among the multiplicity bins, as can be seen in fig 1, which causes a finite range of multiplicities to show the dark blue border in fig 7.

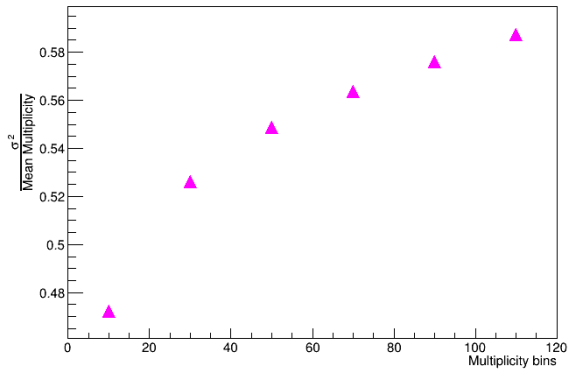

(a) Against Multiplicity bin midpoints

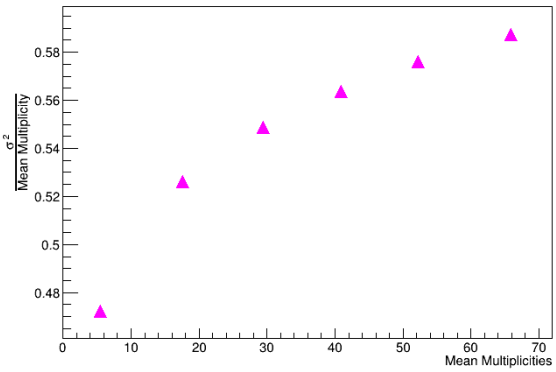

(b) Against mean of Multiplicity ($|\eta| \geq 1$) for each bin

FIG. 11: Variance of Net Charge distributions scaled down by mean of multiplicity estimator ($|\eta| \geq 1$)

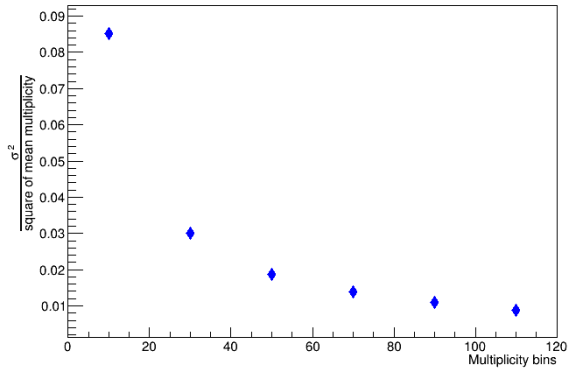

(a) Against Multiplicity bin midpoints

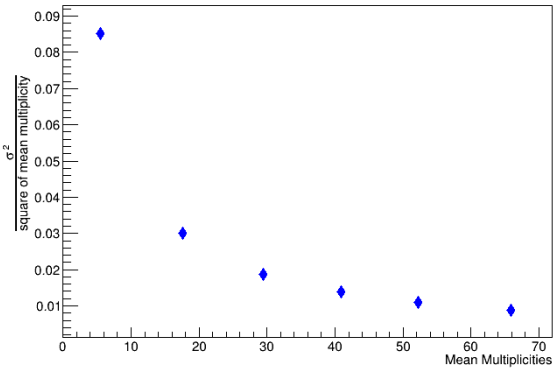

(b) Against mean of Multiplicity ($|\eta| \geq 1$) for each bin

FIG. 12: Variance of Net Charge distributions scaled down by square of mean of multiplicity estimator ($|\eta| \geq 1$)

Whereas $(\frac{\sigma^2}{M_{\rm mult}})$ is increasing with multiplicity, $(\frac{\sigma^2}{M^2_{\rm mult}})$ is decreasing.

III. SUMMARY

The study of the net charge distribution against multiplicity of proton-proton collisions at center-of-mass energy 13 TeV has been presented. The distribution is calculated for $|\eta| < 1$ as the acceptance region, and plotted against the multiplicity estimator, the multiplicity for $|\eta| \geq 1$. The mean and variance of the net charge increase with the multiplicity. The variance scaled down by the mean multiplicity increases with the multiplicity as well, but the variance scaled down by the square of the mean multiplicity decreases. These trends are in good agreement with the corresponding results for heavy-ion (Au-Au) collisions obtained in the reference. The codes and obtained results have been documented here.

REFERENCES

[1] J. Adams *et al.*, (ALICE Collaboration), Nature Physics**13**,535-539 (2017).